Optimizing stored light efficiency in vapor cells

Irina Novikova[a], Mason Klein[a,b], David F. Phillips[a], Ronald L. Walsworth[a,b]

[a]Harvard-Smithsonian Center for Astrophysics, 60 Garden St., Cambridge, MA, USA;
[b]Department of Physics, Harvard University, Cambridge, MA, USA

ABSTRACT

We present a preliminary experimental study of slow and stored light in Rb vapor cells under the conditions of electromagnetically induced transparency (EIT). We study the efficiency of light storage as a function of pulse duration, storage time, retrieval field intensity, etc. We demonstrate that atomic diffusion in-and-out of the laser beam plays an important role not well described by previous analysis.

Keywords: Electromagnetically induced transparency, slow light, stored light, vapor cell, buffer gas

1. INTRODUCTION

Photons are the preferred carriers of information in both classical and quantum communications. Modern optical communication networks rely on strong light pulses to carry information. Quantum networks, in which information is encoded in quantum states of individual photons, would allow absolutely secure communication. An important challenge in such quantum communication is to transmit individual photons over long distances while preserving their individual quantum states. Inevitable losses in optical fibers severely limit the distance between nodes in such a communication channel.

Optical losses in classical communication are corrected for by using optical amplifiers along the transmission line, which restore the amplitude of classical light pulses. This approach, however, is impossible for quantum information transmission. Instead of amplifiers, one needs to distribute quantum repeaters – optical components which "purify" photon states along a transmission line.[1,2] Realization of such repeaters requires the development of a quantum memory that is capable of storing, releasing and manipulating quantum states at the level of individual light quanta.

Such a quantum memory may be realized using the coherent transfer of quantum states of photons to quantum states of atoms.[3] Long-lived atomic states are ideal for storing quantum information. There are several approaches to the realization of photon-atom coherent state transfer. The most theoretically straightforward mechanism is to couple each photon to a single individual atom by coherent absorption and emission.[4] Despite technical difficulties, tremendous progress has been made in this field.[5–7] An alternative approach is to map a photon state into the collective quantum state of an ensemble of many indistinguishable atoms. For example, it is possible to achieve continuous variable quantum state mapping into atomic samples using dispersive light-matter interaction via quantum teleportation.[8–11]

Another promising mechanism for photon state transfer is based on the phenomenon of ultra-slow group velocity propagation of light pulses under the conditions of electromagnetically induced transparency (EIT).[12,13] In this case a strong classical field controls the propagation of weak probe photons through a resonant atomic medium, and creates a strong coupling between probe photons and the collective excitation of atomic spins. By adiabatically reducing the group velocity to zero (by reducing the control field amplitude) the photonic excitation is coherently transferred into the spin excitation. This process is completely reversible, *i.e.*, the original photons can be recreated by turning the control field back on. This process has been predicted[14–16] and experimentally demonstrated for both classical[17–19] and quantum[20–23] regimes of pulse propagation. The light storage technique, described above, is capable of transferring quantum states of light to atomic ensembles and back perfectly only under the condition of no dissipative optical losses and no decay of atomic spin states. In realistic systems, however, the fidelity of the storage is reduced due to various decoherence mechanisms.

The techniques of slow- and stored-light have important applications even for classical optical communication for optical delay lines. For example, light storage is conceptually well-suited for the implementation of all-optical pulse delays, allowing control over the release time of each pulse. To make this technique practical, we must store

Advanced Optical and Quantum Memories and Computing II, edited by Hans J. Coufal, Zameer U. Hasan, Alan E. Craig, Proceedings of SPIE Vol. 5735
(SPIE, Bellingham, WA, 2005) · 0277-786X/05/$15 · doi: 10.1117/12.601709

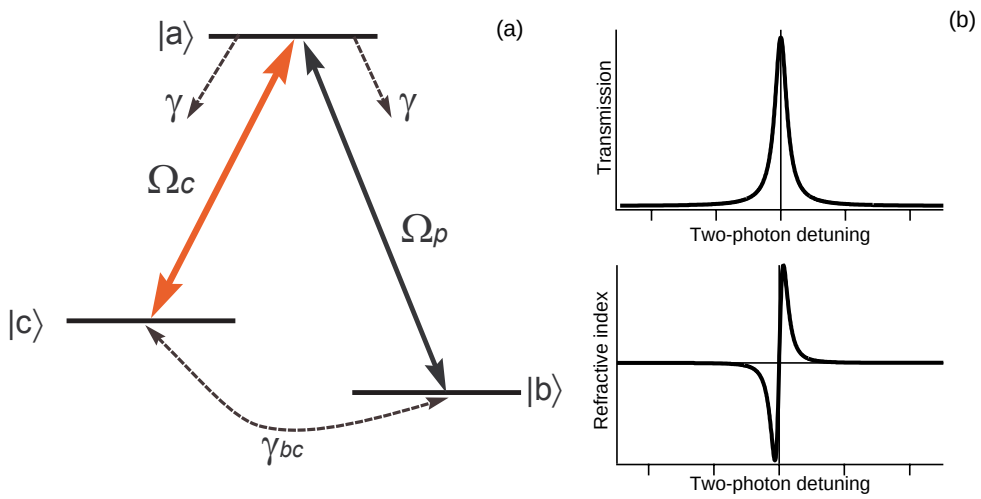

Figure 1. (a) Idealized interaction scheme for the control field Ω_c and probe field Ω_c with three-level atoms in Λ configuration. (b) Transmission and dispersion lineshapes for EIT in a three-level system.

light pulses with high bandwidth for times exceeding the pulse duration and then recreate them with minimal pulse shape distortion.

In order to evaluate stored light techniques for practical applications, it is important to investigate various decoherence mechanisms, and develop techniques to minimize their impact. Ultimately, we want to find a set of experimental conditions that allow the storage and retrieval of classical and quantum optical pulses with high fidelity. Here, we report a preliminary study of the fidelity of light storage in Rb vapor cells filled with neon buffer gas, and characterize the important role played by Rb diffusion in-and-out of the laser beam.

This paper is organized as follows. Section 2 provides a brief summary of the theoretical calculations of pulse propagation under EIT conditions in a three-level Λ system. We describe the details of the experimental apparatus in Section 3. The results of our experiments for slow- and stored-light in a Rb vapor cell with Ne buffer gas is in Section 4. We conclude with Section 5.

2. THEORY FOR SLOW AND STORED LIGHT IN Rb ATOMS

A large number of publications describe the interaction of a probe field with three-level atoms under EIT conditions (see, *e.g.*, Refs. (12, 24) and references therein). Here we briefly summarize the main results for slow- and stored-light which are relevant for our experiments.

Figure 1 shows an idealized three-level atom. We assume that the population of the excited state $|a\rangle$ decays equally into two ground states $|b\rangle$ and $|c\rangle$ with the rate γ. We initially assume no decoherence between the two ground states, *i.e.*, $\gamma_{bc} = 0$. In this case the propagation of a weak probe field of Rabi frequency Ω_p, resonant with one of the allowed optical transitions (for example $|b\rangle \rightarrow |a\rangle$), is completely controlled by the strong field Ω_c (applied to the transition $|c\rangle \rightarrow |a\rangle$). In particular, one can achieve 100% transmission of a probe field if it is in two-photon Raman resonance with the control field due to quantum interference in an effect known as electromagnetically induced transparency.[13, 25] The bandwidth of this transparency window is proportional to the intensity of the control field $\propto |\Omega_c|^2/\gamma$.

The presence of the control field also modifies the refractive index of the atomic medium. Transparency is accompanied by a steep positive dispersion $dn(\nu_p)/d\nu_p$, where ν_p is the frequency of the probe field. This results in ultra-slow group velocities for the probe pulse. If the bandwidth of the pulse lies within the EIT window, then

the pulse will be delayed while propagating through the atomic medium of length L by the group delay τ[12, 13]:

$$\tau = L/v_{gr} = \frac{3}{8\pi} N\lambda^2 L \frac{\gamma}{|\Omega_c|^2}. \quad (1)$$

Here N is the number density of atoms, λ is the probe field wavelength, and γ is the decay rate of the excited state. The intensity of the control field dictates the propagation velocity of the probe pulse: the weaker the field, the longer the group delay. Therefore, by changing the intensity of the control field one is able to control the dynamics of the probe pulse. In particular, reducing the control field intensity to zero reduces the group velocity to zero, storing the pulse in the atomic medium.

It is convenient to describe such slow light propagation in terms of "dark-state polaritons",[14, 16, 24] which treat the propagation of the probe pulse through the EIT medium as a combination of photonic and atomic spin coherence components. This theory provides a simple description of stored light as a dark-state polariton with all excitation in the atomic component. In atoms with negligible ground-state decoherence such a pulse can be stored for an arbitrarily long time and then released by switching the control field back on. Quantum states of pulses so retrieved are identical to those of the input.

In any real atomic system the ground states undergo decoherence, characterized by the rate γ_{bc}. Non-zero γ_{bc} has several effects on stored light. First it leads to residual absorption, under otherwise ideal EIT conditions,[12, 26] given by:

$$|\Omega_p(L)|^2 = |\Omega_p(0)|^2 \exp\left(-\frac{3}{8\pi} N\lambda^2 L \frac{\gamma\gamma_{bc}}{|\Omega_c(0)|^2}\right). \quad (2)$$

Thus some fraction of the probe pulse is absorbed incoherently, and any corresponding information is lost.

Ground-state decoherence also limits the two-photon EIT linewidth in the limit of low control field intensity. In the three-level system of Fig. 1 the EIT resonance is a symmetric Lorentzian function of the two-photon detuning with a width $\gamma_{\rm EIT}$[12, 13]:

$$\gamma_{\rm EIT} = \gamma_{bc} + \frac{|\Omega_c|^2}{\gamma}. \quad (3)$$

During the storage period, information is also lost due to ground-state decoherence at the rate γ_{bc}, leading to limitations on the available storage time and efficiency of the pulse in the medium.

In the experiments reported here, the leading cause of ground-state decoherence is the loss of atoms from the interaction region. Atoms in our vapor cells are at temperatures slightly above room temperature and have thermal velocities of $v_T \approx 3 \times 10^4$ cm/s. To increase the time that atoms spend interacting with the laser fields, a buffer gas is introduced (usually a noble gas or N_2), which restricts the motion of atoms without much effect on their level structure. The most important consequences of the buffer gas are a frequency shift and broadening of both the optical[27] and ground-state microwave[28] transitions. For our experimental conditions (5 Torr of Ne buffer gas) we can neglect any dephasing of the ground-state coherence due to collisions with buffer gas atoms. Then one can expect for the ground-state coherence decay rate γ_{bc} in a buffer gas cell to be inversely proportional to the diffusion time τ_d of an atom through the laser beam. We can find this time under the approximation of small laser beam diameter ($a \ll A$, where a and A are the diameters of the laser beam and the atomic cell correspondingly)[29, 30]:

$$\frac{1}{\tau_d} = 2.405^2 \frac{D}{a^2} \frac{1}{1 + 6.8\lambda/a} \quad (4)$$

where D is the diffusion coefficient, $\lambda = 3D/v_T$ is the mean free path, and v_T is the average thermal velocity of the Rb atoms.

In our measurements with a buffer gas consisting of 5 Torr of Ne, the diffusion constant $D = 76$ cm^2/s, and $\lambda = 0.06$ mm. Using Eq. (4) we estimate that the diffusion time of a Rb atom through a laser beam of diameter $a \approx 0.8$ mm is $\tau_d \approx 7$ μs, which corresponds to a ground-state linewidth of $\gamma_{bc}/\pi \approx 45$ kHz.

This approach, however, oversimplifies the process of atomic diffusion. The distribution of coherence in the full volume of the vapor cell must be accounted for to realistically describe observed EIT lineshapes and the dynamics of probe pulse propagation.

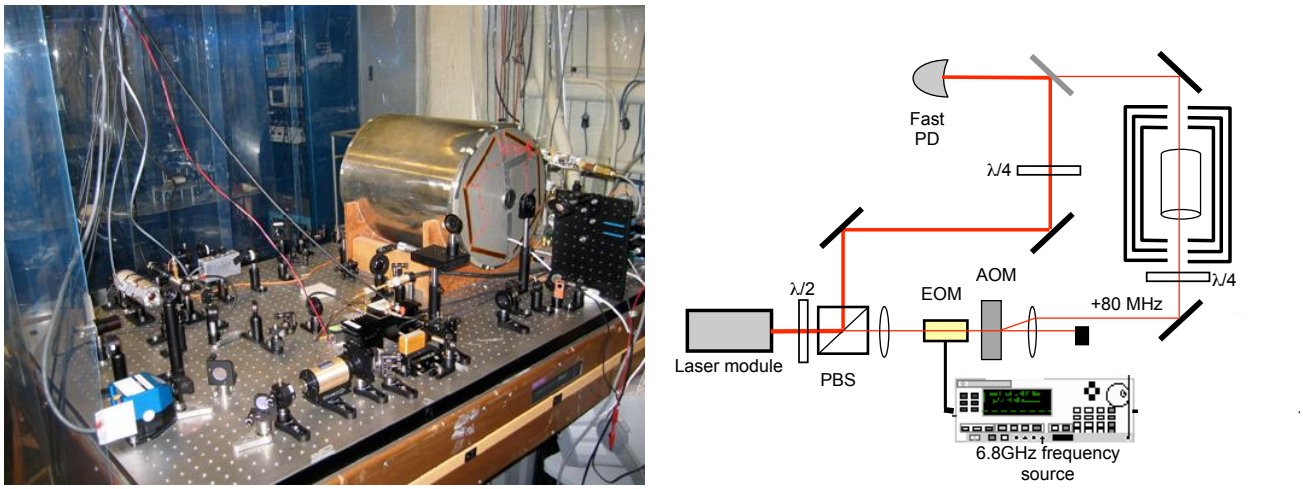

Figure 2. Schematic and photograph of the experimental setup. See text for definitions.

3. APPARATUS

The schematic of the experimental setup is shown in Fig. 2. We used a commercial external cavity diode laser[31] tuned in the vicinity of the $5^2S_{1/2} \rightarrow 5^2P_{1/2}$ (D_1) line of ^{87}Rb. Total available laser power was about 13 mW. We split the laser beam using a polarizing beam splitter (PBS), creating a reference beam which did not go through the rest of the optical system. We modulated the phase of the main laser field at 6.835 GHz using an electro-optical modulator (EOM)[32] to produce a probe field. Since the RF modulation index was quite small ($\epsilon \leq 0.03$) only $\approx 2\%$ of total light power was transferred to each first order sideband and the amplitude of higher sidebands was negligibly small. All three optical fields then passed through an acousto-optical modulator (AOM), shifting the frequencies of all fields by +80 MHz. Gaussian-shaped probe pulses of various durations and amplitudes were created by amplitude modulation of the RF-frequency synthesizer driving the EOM, while the total power of the control and probe fields was controlled by changing the amplitude of the AOM, allowing for fast switching times. During light storage measurements, power to the EOM was clamped to zero after the writing period, ensuring that no input probe field was present during the retrieval period.

Before entering the vapor cell the laser beam was weakly focused to a 0.8 mm diameter spot and circularly polarized using a quarter-wave plate ($\lambda/4$). The cell containing isotopically enriched ^{87}Rb and 5 Torr of Ne buffer gas was mounted inside a three-layer magnetic shield, which allowed for compensation of stray magnetic fields to less than 30 μG over the interaction region. We controlled the temperature of the cell using a blown-air oven; for the measurements described below the temperature was maintained at 65°C. We tuned the laser such that the main carrier frequency field was resonant with $F = 2 \rightarrow F' = 2$ transition of ^{87}Rb; in this case the +1 sideband was resonant with $F = 1 \rightarrow F' = 2$ transition. In this work we neglected any influence of the far-detuned −1 sideband.

After traversing the cell, the laser beam was combined with the reference beam on a 50/50 beam-splitter and sent to a fast photodetector.[33] Since the frequency of the reference field is shifted 80 MHz down from the control field, we can detect the +1 sideband by measuring the amplitude of the beat note at 6.915 GHz using a spectrum analyzer in zero-span mode (resolution bandwidth 300 kHz).

4. EXPERIMENTAL RESULTS

We can divide the storage process into three steps: (i) propagation of the pulse as slow light; (ii) storage of the probe pulse as a spin coherence wave; and (iii) retrieval of the probe pulse. We will discuss the optimization of the parameters for each step. Since the range of experimental parameters is very broad, we will concentrate of just a few: control and probe field powers and probe pulse duration. In future work we will explore the

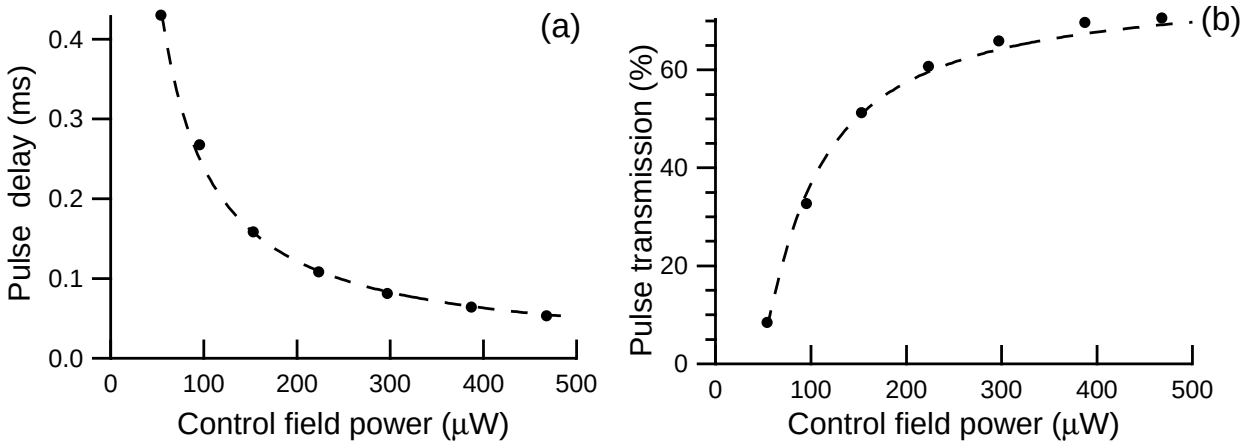

Figure 3. (a) Delay of the probe pulse propagating through the Rb cell under slow light conditions as a function of the control field power P_c; the dashed line is the best fit of the experimental points given by Eq. (1). (b) Transmitted amplitude of the probe pulse versus control field power; the dashed line is the best fit of the experimental points given by Eq. (2). The probe pulse has a Gaussian form with a FWHM ≈ 1 ms.

dependence of buffer gas pressure and composition, laser beam diameter, one-photon detuning of the probe and control fields, etc. on the stored light efficiency. We also must note some relevant studies of slow group velocity propagation in Rb vapor in the presence of buffer gases as a function of atomic density and buffer gas pressure, which provide some insights on the optimal parameters for the light storage process.[34]

4.1. Optimization of the control field power

In the first stage of light storage, the probe pulse is compressed into the atomic medium of length given by the vapor cell. To store the full pulse in the atomic medium, it must be delayed for at least one temporal width of the original pulse. Experimental conditions must be found which allow the probe pulse to be delayed by its full length or the leading edge of the pulse will exit the cell while the control field is still on.

Reduction of the group velocity by reducing the control field power or increasing the atomic density (see Eq. (1)), is accompanied by increasing optical losses due to both reduced EIT quality (Eq. (2)) and bandwidth (Eq. (3)). Figure 3a shows the probe pulse delay scaling as the inverse of the control field intensity. Corresponding to the increased delay is a reduction in transmitted pulse power (Fig. 3b). These results are in good agreement with Eqs. (1) and (2). Propagation of the pulse is unaffected by the probe field intensity (for intensities weak compared to the control field) as would be expected from the theory described above. Control field power must therefore be adjusted to balance pulse delay and transmission for optimized light storage.

Figure 4 shows the light storage process for various storage times and two different values of the writing control field power. For a low control field power (50 μW), we capture the whole pulse inside the cell (Fig. 4b). At a stronger control field power (150 μW), the group velocity is higher and a significant fraction of the input probe pulse escapes from the atomic medium before the light is turned off (Fig. 4a). Slightly smaller retrieved pulse amplitudes are observed at weaker write control fields, however, due to larger incoherent losses during both the write and retrieval stages (see Fig. 5).

We therefore define the efficiency of light storage as the ratio of the area of the retrieved pulse to the area of the input pulse. This definition of storage efficiency does not distinguish between losses associated with: (a) the attenuation of the probe pulse due to residual absorption; (b) losses during the storage period; and (c) escape of the input pulse during the write process if the group velocity is not low enough. The efficiency of the retrieved pulses is plotted as a function of the storage time in Fig. 5. For both the strong and weak control fields during the write process, the efficiency decays exponentially with time, most likely due to the decay of atomic spin

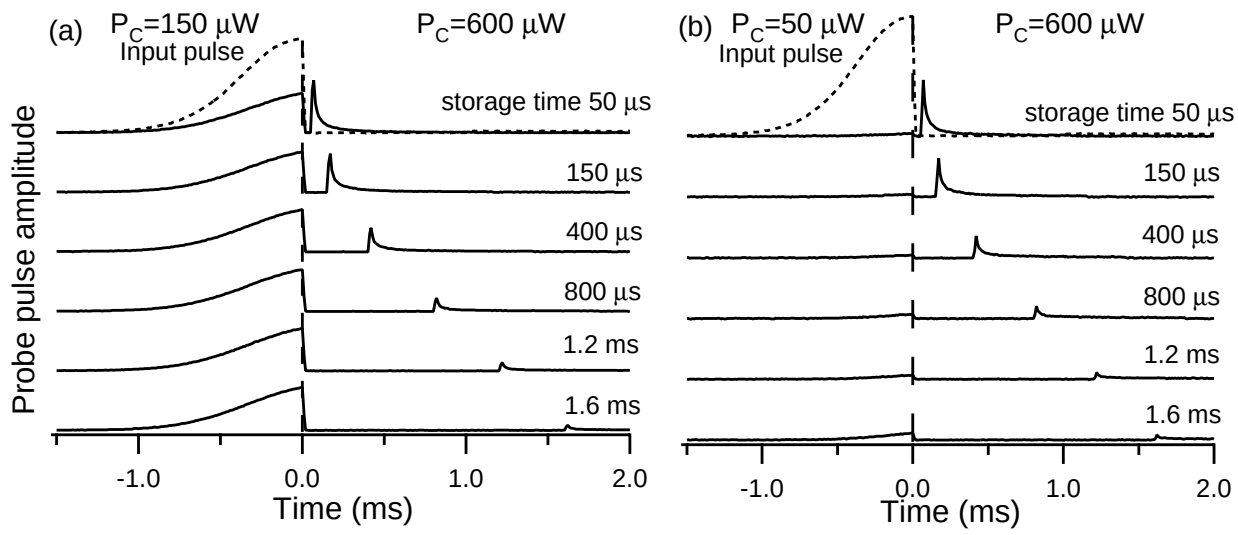

Figure 4. Light storage for various storage intervals and two control field powers during the write process: (a) 150 μW and (b) 50 μW. The input pulse duration (dashed line) is 500 μs and the retrieve control power is 600 μW for all measurements. Variations in the amplitude of the leading (slow light) pulse are due to drifts of the laser frequency, which affects the group velocity of the probe pulses.

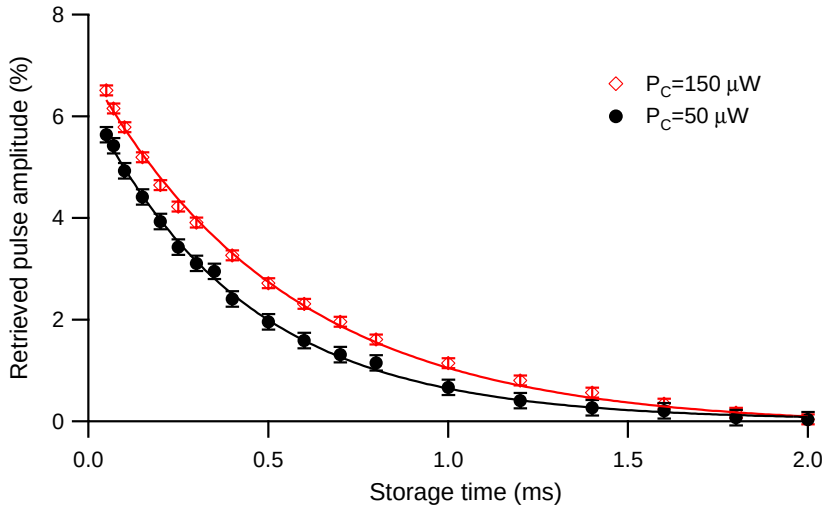

Figure 5. The ratio of the retrieved probe pulse area to the input pulse area (the efficiency as defined in the text) as a function of the storage time for two different write control fields: 50 μW ($\bullet$) and 150 μW ($\diamond$). The $1/e$ decay times from exponential fits (solid lines) are respectively 430 μs and 550 μs.

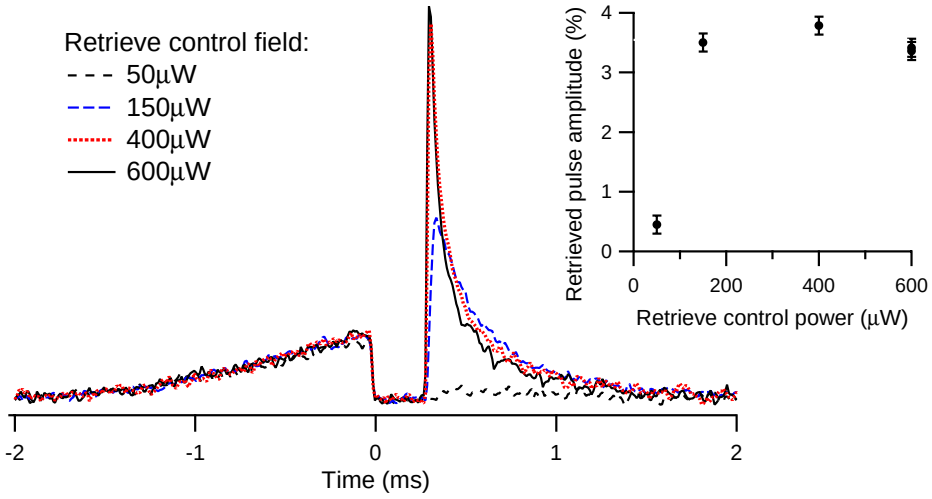

Figure 6. Retrieved pulse at several retrieve control field intensities. The storage time is 300 μs and the intensity of the control field during the writing stage is 50 μW. *Inset*: the retrieved probe pulse area normalized to the input pulse area as a function of the retrieve control field.

coherence. The decay time in both cases is approximately 500 μs and retrieved pulses are observed for storage times up to 2 ms. Note that these times are much longer than the diffusion-limited ground-state coherence lifetime given by Eq. (4), as we will discuss in the next subsection.

The shape of the original output pulse is only preserved if the control field parameters during the retrieval stage are identical to those of the writing stage.[14, 16] Larger intensities during the retrieval process lead to higher probe field group velocities and thus compressed output pulses (Fig. 6). Similar behavior is observed in the few-photon pulse regime as well.[22] Despite the compression, the area of the output pulse is preserved provided that the EIT bandwidth is large compared to the intrinsic linewidth, which is the case in all but the smallest of our retrieval control fields (inset of Fig. 6). In principle, short, strongly compressed pulses are less susceptible to losses during the retrieval process from atomic decoherence as well as smaller analysis uncertainties associated with background correction. Therefore, the control field power is kept at 600 μW for the measurements reported here.

4.2. Optimization of the probe field pulse duration

Large fractional delays may also be obtained by shortening the input pulse. The absolute time delay should remain unchanged as the pulse is shortened (Eq. (1)), provided that the bandwidth of the pulse is smaller than the EIT width given by Eq. (3). For shorter pulses both the group velocity and optical losses increase because the probe pulse contains frequency components outside the EIT transparency window which do not propagate under slow light conditions.

The minimum EIT bandwidth will be set by the ground-state decoherence rate (Eq. (3)). Atomic diffusion is the dominant mechanism for ground-state decoherence. The time for atoms to diffuse out of the laser beam given by Eq. (4) is approximately 7 μs for our buffer gas and beam diameter. Therefore, pulses longer than 10 μs might be expected to propagate with constant group velocity, as the pulse length is increased. We observe (Fig. 7), however, that pulse delays only saturate for pulse lengths with durations of several milliseconds: one hundred times longer than these simple considerations would suggest. Additionally, for pulses shorter than one millisecond, we observe distortion of the pulse shape, suggesting that even though the bandwidth of the pulse is much smaller than the EIT bandwidth, both absorption and dispersion depend strongly on two-photon detuning.

Similar effects are also be observed in static measurements of probe field transmission as a function of two-photon detuning (Fig. 8). The lineshape is not a Lorentzian as expected in the three-level Λ system model. While

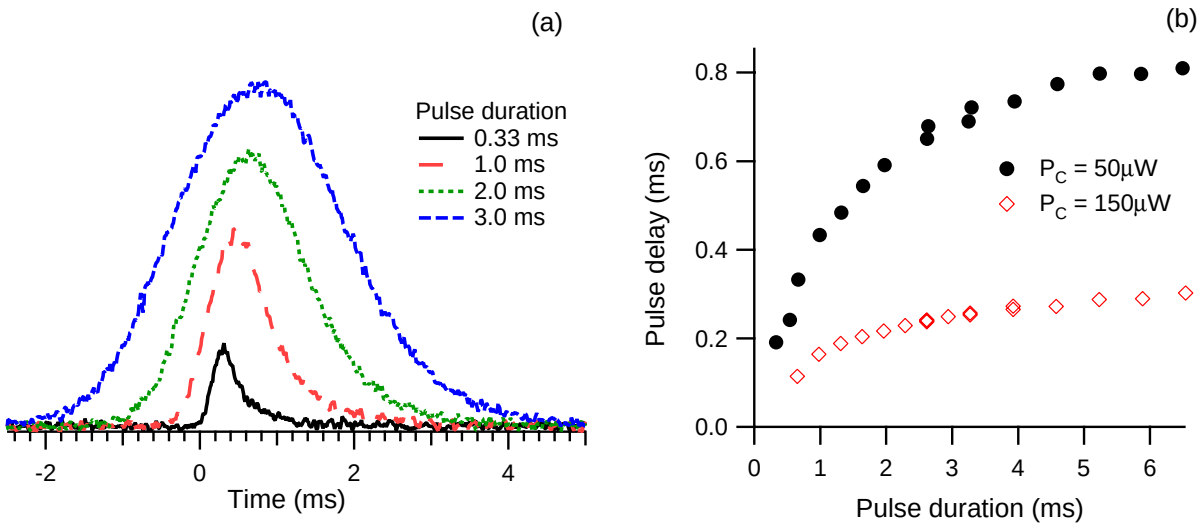

Figure 7. (a) Transmitted slow light pulses for various pulse durations. Input pulse amplitudes are equal. ($P_c \approx 50\mu$W.) (b) Group delay as a function of pulse duration.

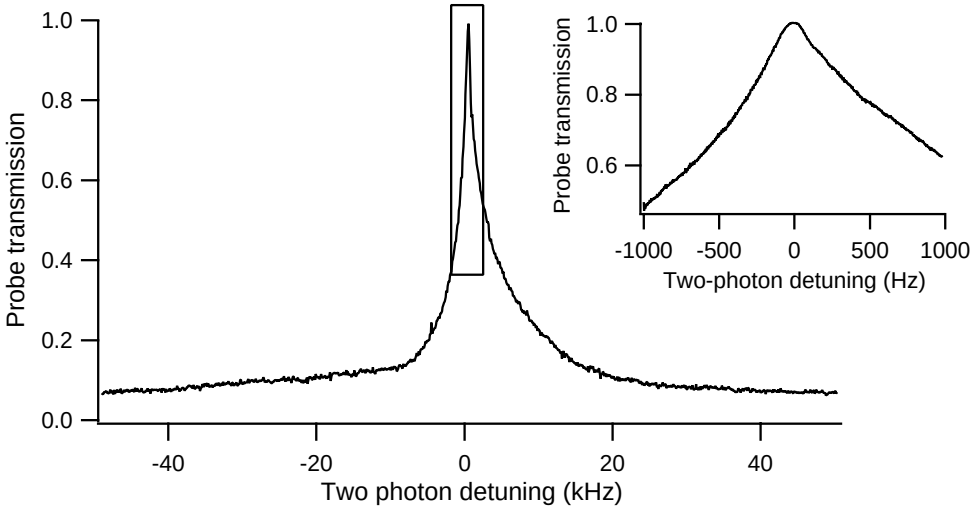

Figure 8. Probe transmission as a function of two photon detuning (*i.e.*, EOM drive frequency). *Inset*: Central region of the resonance. ($P_c \approx 150$ μW.) The amplitude of the peak is normalized to the maximum transmission under EIT conditions. Some asymmetry of the resonances is due to drift of the laser from the atomic resonance.

the overall width appears to be consistent with that expected from diffusion of the atoms out of the laser beam, the central structure is significantly narrower. Calculations taking into account the inhomogeneous (Gaussian) transverse distribution of the laser beam[35,36] also fail to reproduce the observed EIT lineshape and its sharp central region.

The model described in Sec. 2, however, assumes that a Rb atom which enters the interaction region spends a mean time τ_d there and then leaves, never returning to the interaction region with any coherence. In a more detailed model of atomic diffusion in the vapor cell, an atom has nonzero probability of returning to the interaction region *before* its coherence is destroyed as a result of a collision with the vapor cell wall or multiple

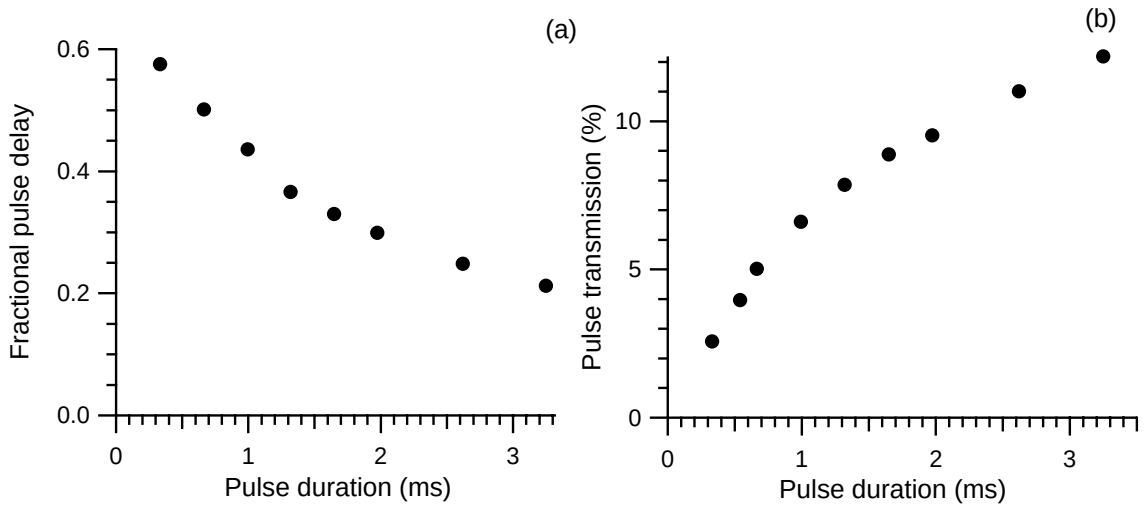

Figure 9. Slow light (a) fractional delay and (b) transmission as a function of input pulse length. ($P_c \approx 50$ μW.)

collisions with buffer gas atoms or molecules. For such atoms, the ground-state coherence lifetime may be much longer and power broadening will be reduced since the atoms spend most of their time outside of the laser beam. Thus, it is reasonable to conclude that such atoms produce the narrow spectral feature observed in the EIT resonance. Note that this sharp peak in the transmission resonance corresponds to a steep nonlinear variation in the refractive index in the small frequency range near the center of the resonance.

The narrow transmission component leads to the several millisecond storage times (see Figs. 4 and 5) while the steep, near-resonance component of the index of refraction leads to long absolute delay times (Fig. 7b). For high efficiency light storage, we need large *fractional* delays. Figure 9 shows the dependence of the fractional delay (the ratio of the time delay to the $1/e$ full temporal width of the pulse) and the fractional transmission. We find that the fractional pulse time delay falls more slowly than would be expected from simple theory (Eq. 1, 3 and 4) due to diffusion in-and-out of the beam. Considering optical losses as well, the optimal value of the probe pulse is approximately 1 ms. Finally, the stored light efficiency as a function of the pulse duration reaches its maximum for $1-2$ ms pulses (Fig. 10) and then slowly decreases as is expected from the slow light fractional delay results.

5. CONCLUSION

We have studied the optimization of slow- and stored-light propagation in a warm Rb vapor cell in the presence of a Ne buffer gas. The adjustment of the control field power during both the writing and retrieving stages of stored light are in a good agreement with existing models.[14, 16, 22] An optimal value of the control field must be found to achieve a large compression of the pulse inside the atomic medium without large optical losses associated with imperfect EIT. Additionally, the presence of a buffer gas changes the spectral lineshape of the EIT resonance, making atomic susceptibility very sensitive to detuning from two-photon resonance and pulse delays dependent on pulse duration for long pulses. We attribute this to the diffusion of coherently-prepared atoms in-and-out of the laser beam and thereby increasing the average coherence lifetime by more than an order of magnitude. This also restricts the duration of pulses which can be stored without distortion. Future improvements in light storage efficiency will be sought through continued studies, such as the dependence of fidelity upon buffer gas pressure, beam diameter and density-length product of Rb in the vapor cell.

6. ACKNOWLEDGEMENTS

The authors are grateful to M.D. Lukin, M. D. Eisaman, L. Childress, A. André, M. Crescimanno, and A. S. Zibrov for useful discussions. This work was supported by DARPA, ONR and the Smithsonian Institution.

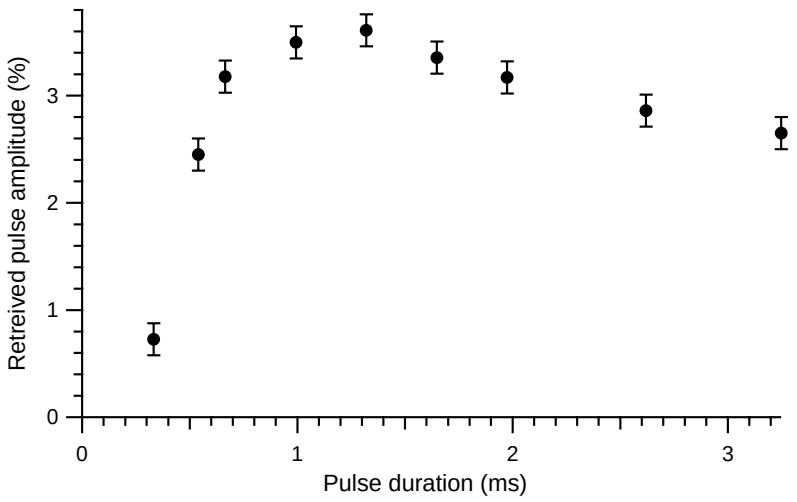

Figure 10. Retrieved pulse area normalized to input pulse area as a function of pulse duration. The control field power (P_c) during the writing stage is 50 μW, and is 600 μW during the retrieval stage. The storage time is 100 μs.

REFERENCES

1. H.-J. Briegel, W. Dur, J. I. Cirac, and P. Zoller, "Quantum repeaters: The role of imperfect local operations in quantum communication," *Phys. Rev. Lett.* **81**, pp. 5932–5935, 1998.
2. D. Bouwmeester, A. Ekert, and A. Zeilinger, *The Physics of Quantum Information*, Springer, New York, 2000.
3. L. M. Duan, M. D. Lukin, J. I. Cirac, and P. Zoller, "Long-distance quantum communication with atomic ensembles and linear optics," *Nature* **414**, pp. 413–418, 2001.
4. H. J. Kimble, "Strong interactions of single atoms and photons in cavity QED," *Phys. Scr.* **76**, pp. 127–137, 1998.
5. A. Kuhn, M. Hennrich, and G. Rempe, "Deterministic single-photon source for distributed quantum networking," *Phys. Rev. Lett* **89**, p. 067901, 2002.
6. J. McKeever, A. Boca, A. D. Boozer, J. R. Buck, and H. J. Kimble, "Experimental realization of a one-atom laser in the regime of strong coupling," *Nature* **425**, pp. 268–271, 2003.
7. J. McKeever, A. Boca, A. D. Boozer, R. Miller, J. R. Buck, A. Kuzmich, and H. J. Kimble, "Deterministic generation of single photons from one atom trapped in a cavity," *Science* **303**, pp. 1992–1994, 2004.
8. A. E. Kozhekin, K. Mølmer, and E. S. Polzik, "Quantum memory for light," *Phys. Rev. A* **62**, p. 033809, 2000.
9. B. Julsgaard, J. Sherson, J. I. Cirac, J. Fiurášek, and E. S. Polzik, "Experimental demonstration of quantum memory for light," *Nature* **432**, pp. 482–486, 2004.
10. K. Hammerer, K. Mølmer, E. S. Polzik, and I. J. Cirac, "Light-matter quantum interface," *Phys. Rev. A* **70**, p. 044304, 2004.
11. J. Fiurášek, N. J. Cerf, and E. S. Polzik, "Quantum cloning of a coherent light state into an atomic quantum memory," *Phys. Rev. Lett.* **93**, p. 180501, 2004.
12. M. O. Scully and M. S. Zubairy, *Quantum Optics*, Cambridge University Press, Cambridge, UK, 1997.
13. S. E. Harris, "Electromagnetically induced transparency," *Phys. Today* **50**, pp. 36–39, July 1997.
14. M. Fleischhauer and M. D. Lukin, "Dark-state polaritons in electromagnetically induced transparency," *Phys. Rev. Lett.* **84**, pp. 5094–5097, 2000.
15. M. Fleischhauer, S. F. Yelin, and M. D. Lukin, "How to trap photons? storing single-photon quantum states in collective atomic excitations," *Opt. Commun.* **179**, pp. 395–410, 2000.

16. M. Fleischhauer and M. D. Lukin, "Quantum memory for photons: Dark-state polaritons," *Phys. Rev. A* **65**, p. 022314, 2002.
17. C. Liu, Z. Dutton, C. H. Behroozi, and L. V. Hau, "Observation of coherent optical information storage in an atomic medium using halted light pulses," *Nature* **409**, pp. 490–493, 2001.
18. D. F. Phillips, A. Fleischhauer, A. Mair, R. L. Walsworth, and M. D. Lukin, "Storage of light in atomic vapor," *Phys. Rev. Lett.* **86**, pp. 783–786, 2001.
19. A. Mair, J. Hager, D. F. Phillips, R. L. Walsworth, and M. D. Lukin, "Phase coherence and control of stored photonic information," *Phys. Rev. A* **65**, p. 031802, 2002.
20. C. H. van der Wal, M. D. Eisaman, A. Andre, R. L. Walsworth, D. F. Phillips, A. S. Zibrov, and M. D. Lukin, "Atomic memory for correlated photon states," *Science* **301**, pp. 196–200, 2003.
21. A. Kuzmich, W. P. Bowen, A. D. Boozer, A. Boca, C. W. Chou, L. M. Duan, and H. J. Kimble, "Generation of nonclassical photon pairs for scalable quantum communication with atomic ensembles," *Nature* **423**, pp. 731–734, 2003.
22. M. D. Eisaman, L. Childress, A. Andre, F. Massou, A. S. Zibrov, and M. D. Lukin, "Shaping quantum pulses of light via coherent atomic memory," *Phys. Rev. Lett.* **93**, p. 233602, 2004.
23. D. N. Matsukevich and A. Kuzmich, "Quantum state transfer between matter and light," *Science* **306**, pp. 663–666, 2004.
24. M. D. Lukin, "Colloquium: Trapping and manipulating photon states in atomic ensembles," *Rev. Mod. Phys.* **75**, pp. 457–472, 2003.
25. J. P. Marangos, "Electromagnetically induced transparency," *J. Mod. Opt.* **45**, pp. 471–503, 1998.
26. H. Lee, Y. Rostovtsev, C. J. Bednar, and A. Javan, "From laser induced line narrowing to electromagnetically induced transparency: closed system analysis," *Appl. Phys. B* **76**, pp. 33–39, 2003.
27. C. Ottinger, R. Scheps, G. W. York, and A. Gallagher, "Broadening of Rb resonance lines by noble-gases," *Phys. Rev. A* **11**, pp. 1815 –1828, 1975.
28. J. Vanier, J.-F. Simard, and J.-S. Boulanger, "Relaxation and frequency shifts in the ground state of Rb^{85}," *Phys. Rev. A* **9**(3), pp. 1031–1040, 1974.
29. W. Happer, "Optical pumping," *Rev. Mod. Phys.* **44**, pp. 169–249, 1972.
30. E. Arimondo, "Relaxation processes in coherent-population trapping," *Phys. Rev. A* **54**, pp. 2216 –2223, 1996.
31. New Focus Vortex laser model 6017.
32. New Focus phase modulator model 4431.
33. New Focus 12-GHz Broadband Photoreceiver Model 1554-A.
34. E. E. Mikhailov, Y. Rostovtsev, and G. R. Welch, "Group velocity study in hot Rb-87 vapour with buffer gas," *Journal of Modern Optics* **50**(14/15), pp. 2645–2654, 2003.
35. E. Pfleghaar, J. Wurster, S. Kanorsky, and A. Weis, "Time of flight effect in nonlinear magneto-optical spectroscopy," *Opt. Commun.* **99**, pp. 303–308, 1993.
36. A. V. Taichenachev, A. M. Tumaikin, V. I. Yudin, M. Stahler, R. Wynands, J. Kitching, and L. Hollberg, "Nonlinear-resonance line shapes: Dependence on the transverse intensity distribution of a light," *Phys. Rev. A* **69**, p. 024501, 2004.